Experimental Cell Research 387 (2020) 111807

Contents lists available at ScienceDirect

Experimental Cell Research

journal homepage: www.elsevier.com/locate/yexcr

Mechanical strength determines Ca^{2+} transients triggered by the engagement of β_2 integrins to their ligands

Xinyu Shu[a,b,1], Ning Li[a,b,1], Dandan Huang[a,b], Yan Zhang[a,b], Shouqin Lü[a,b], Mian Long[a,b,*]

[a] Center for Biomechanics and Bioengineering, Key Laboratory of Microgravity (National Microgravity Laboratory), Beijing Key Laboratory of Engineered Construction and Mechanobiology, Institute of Mechanics, Chinese Academy of Sciences, Beijing, 100190, China
[b] School of Engineering Sciences, University of Chinese Academy of Sciences, Beijing, 100049, China

ARTICLE INFO

Keywords:
β_2 integrin
Ligands
Calcium transients
Bond strength
Mechanotransduction
Shear stress

ABSTRACT

Lymphocyte function-associated antigen-1 (LFA-1) and macrophage-1 antigen (Mac-1) are key adhesion receptors to mediate neutrophil (PMN) recruitment and intracellular calcium (Ca^{2+}) signaling. Binding of LFA-1 and Mac-1 to their ligands is essential in triggering Ca^{2+} transients and activating Ca^{2+}-dependent kinases involved in cytoskeletal remodeling and migratory function. While mechanical forces are critical in regulating integrin-mediated Ca^{2+} transients, it is still unclear how the bond strength of β_2-integrin-ligand pair affects Ca^{2+} responses. Here three typical ligands with known mechanical features with LFA-1 and Mac-1 in our previous work were adopted to quantify their capabilities in inducing Ca^{2+} transients in adherent PMNs under shear flow. Data indicated that LFA-1 dominates Ca^{2+} transients in PMNs on intercellular adhesive molecule 1 (ICAM-1) and junctional adhesion molecule-A (JAM-A), while Mac-1 mediates Ca^{2+} transients induced by receptor for advanced glycation end products (RAGE), consistent with their corresponding bond strengths. These results link β_2 integrin-ligand bond strength with Ca^{2+} transients in PMNs, suggesting high bond strength gives rise to strong Ca^{2+} response especially under physiological-like shear flow. The outcomes provide a new insight in understanding the mechanical regulatory mechanisms of PMN recruitment.

1. Introduction

Polymorphonuclear leukocytes (PMNs), also known as neutrophils, play an essential role in the innate immune system by initiating killing or repair mechanisms at the site of infection or tissue injury [1]. PMNs circulating in the blood are recruited to the inflammatory sites through a well-defined multistep cascade mediated by specific adhesion molecules and their ligands [2,3]. Two β_2 integrin members, lymphocyte function-associated antigen-1 (LFA-1, $\alpha_L\beta_2$, CD11a/CD18) and macrophage-1 antigen (Mac-1, $\alpha_M\beta_2$, CD11b/CD18) are key adhesion receptors in this process to initiate both adhesive bond formation and intracellular signals [4]. Multiple β_2 integrin ligands are presented on the surface of an endothelial cell (EC), including intercellular cell adhesion molecule 1 (ICAM-1), junctional adhesion molecule A (JAM-A) and receptor for advanced glycation end products (RAGE), promoting PMN adhesion, crawling and transmigration in different tissues [3,5]. While the respective roles of binding these ligands to β_2 integrins are extensively investigated, it is not completely clear how these ligands initiate diverse intracellular signaling under blood flow.

Calcium (Ca^{2+}) response is one of the major signaling triggered by β_2 integrin binding. The cytosolic free Ca^{2+} level contributes to key cellular responses in PMNs including activation, chemotaxis, degranulation and phagocytosis [6]. Ca^{2+} mediates PMN activation during recruitment through its central role in downstream signaling of chemokine ligation and adhesion function [7], and modulates vesicular integrin recycling, cytoskeletal rearrangements and uropod retraction during PMN migration [1]. Moreover, Ca^{2+} regulates the production of reactive oxygen species through activation of the NADPH oxidase *via* Ca^{2+}-dependent protein kinase C and promotes tumor necrosis factor-induced degranulation [1]. Changes in the spatiotemporal distribution of intracellular Ca^{2+} concentration are highly related with PMN behaviors and can be mediated by several ligand-receptor interactions such as the engagement of G-protein coupled receptors (GPCRs), Fcγ-receptors (FcγRs), selectins and integrins [8,9]. Ca^{2+} dynamics of individual PMNs is closely associated with their respective functional states, along with phenotypic changes from one cell state to another [1]. Ca^{2+} transients following PMN adhesion are the cause of cytoskeletal arrangement and cell spreading [10]. In migrating PMNs, Ca^{2+}

* Corresponding author. Institute of Mechanics, Chinese Academy of Sciences, Beijing, 100190, China.
E-mail address: mlong@imech.ac.cn (M. Long).
[1] The authors contributed equally to this work.

https://doi.org/10.1016/j.yexcr.2019.111807
Received 30 October 2019; Received in revised form 26 December 2019; Accepted 27 December 2019
Available online 28 December 2019
0014-4827/

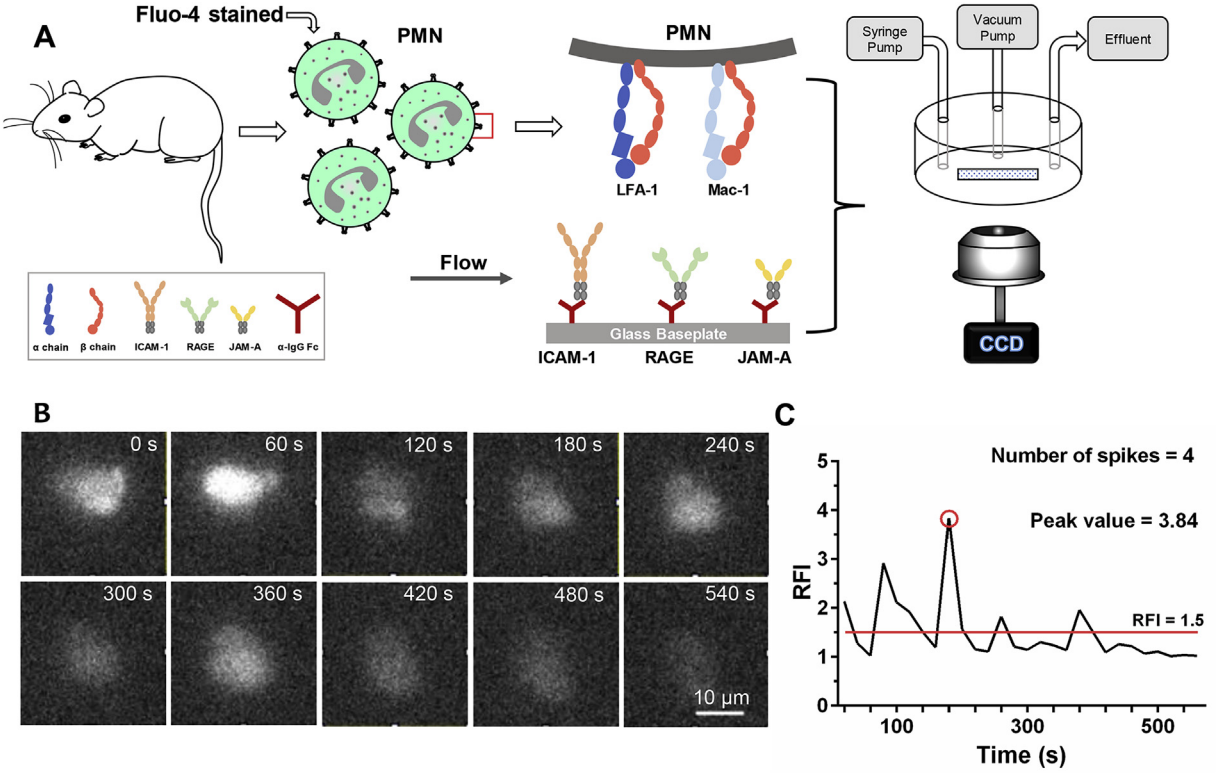

Fig. 1. Real-time fluorescence imaging of intracellular Ca^{2+} in PMNs under shear flow. (*A*) Schematic of experimental set-up (not in scale). BM PMNs were freshly isolated from C57BL/6 mice, loaded with fluo-4-AM, and perfused into the flow chamber with ICAM-1, RAGE or JAM-A-coated substrate. (*B*) Time-lapsed fluorescent images of a stained PMN were recorded to visualize Ca^{2+} transients. (*C*) Typical *RFI* versus time curve reflecting Ca^{2+} transients in a PMN. A *RFI* threshold value of 1.5 was set to define the remarkable Ca^{2+} spikes, and the number of Ca^{2+} spikes and maximum value of peaked *RFI* (peak value) was estimated from the curve.

enriches at the leading edge of pseudopod projection and directs localized cytoskeletal activation and cell migration [8,11]. Meanwhile, binding of LFA-1 and Mac-1 to their ligands is essential in triggering Ca^{2+} transients and activation of Ca^{2+}-dependent kinases involved in cytoskeletal remodeling and migratory function [12–15]. Therefore, the correlation between mechanical loading of integrins and intracellular Ca^{2+} transients is of great interest to understand the mechanotransduction during PMN recruitment [7].

Mechanical forces are critical regulators in integrin-mediated Ca^{2+} transients. Our recent study indicates that mechanical features of ECs affect PMN Ca^{2+} response, and such stiffness-dependent Ca^{2+} response is associated with β_2 integrin activation [16]. Ca^{2+} influx is shear-dependent in rolling PMNs, and contributes to β_2 integrin adhesion and subsequent cell polarization [7]. Shear forces of blood flow transmitted through high-affinity LFA-1 induce their colocalization with Ca^{2+} channel Orai1 and activate a local bursting of Ca^{2+} concentration [11,17]. Tensile forces exerted on cells are balanced by the adhesive forces generated by integrin-ligand interactions during PMN adhesion and migration [18]. However, it is still unclear how mechanical forces of integrin-ligand bonds affect Ca^{2+} signaling in PMNs.

In a previous work, we have quantified the mechanical features of various LFA-1– or Mac-1–ligand bonds [19]. We found that the mechanical strength for LFA-1–ICAM-1/JAM-A bonds are much higher than those for Mac-1–ICAM-1/JAM-A bonds and Mac-1–RAGE bonds are stronger than LFA-1–RAGE bonds. Here we hypothesized that distinct bond strengths of β_2 integrin-ligand pair govern their ligand diversity in regulating Ca^{2+} transients. We compared the capabilities of LFA-1 and Mac-1 to induce Ca^{2+} transients in adherent PMNs on various ligands under static or shear flow conditions and discussed the correlation between bond strength and outside-in signaling.

2. Materials and methods

2.1. Antibodies and reagents

Soluble mouse ICAM-1, RAGE and JAM-A with human IgG Fc chimeras were from R&D Systems (Minneapolis, MN). LEAF™ purified rat anti-mouse CD11a (M17/4) and CD11b (M1/70) blocking monoclonal antibodies (mAbs) and isotype-matched irrelevant control (RTK2758, RTK4530) mAbs were obtained from Biolegend (San Diego, CA). Fluorescent Ca^{2+} indicator Fluo-4 AM (F14201) and solubilizer Pluronic™ F-127 (P3000MP) were from Invitrogen (Carlsbad, CA). Goat anti-human IgG Fc polyclonal antibodies (pAbs), bovine serum albumin (BSA), and chemotactic peptides N-Formyl-Met-Leu-Phe (fMLF) were all from Sigma-Aldrich (St. Louis, MO).

2.2. Murine PMN isolation

All the animal tests were granted permission by the Institutional Animal and Medicine Ethical Committee (IAMEC) at the Institute of Mechanics, Chinese Academy of Sciences. Bone marrow (BM) PMNs were freshly isolated from total 16 male C57BL/6 mice supplied by Vital River Laboratories (Beijing, China) as previously described [20–24]. The experiments were conducted separately with young, sexually mature, 8–12-week mice to provide healthy and functionally competent PMNs. The BM cells were collected from flushing femurs and tibias of both hind legs with Dulbecco's phosphate-buffered saline (DPBS) supplemented with 0.5% BSA and 2 mM EDTA. The cell suspension was filtrated by a 70-μm pore size cell strainer (BD Biosciences, Franklin Lakes, NJ), followed by centrifugation at 300 × *g* for 10 min. Sedimental cells were resuspended in DPBS and isolated by an equilibrium centrifugation of Ficoll-Hypaque density gradient (Histopaque-

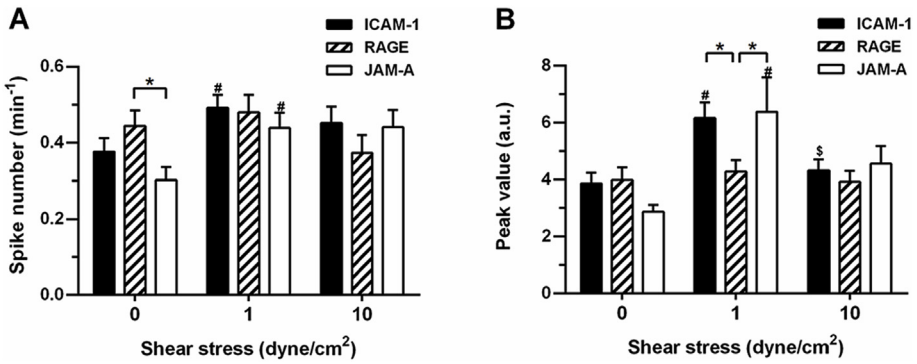

Fig. 2. Intracellular Ca^{2+} transients in adherent PMNs on distinct ligands under static or shear flow conditions. (*A*) Number of Ca^{2+} spikes per minute in PMNs on ICAM-1, RAGE, or JAM-A. (*B*) Peak value of *RFI* in PMNs on ICAM-1, RAGE, or JAM-A. Data are presented as the mean ± SEM from a total of 22–59 cells in 12 FOVs of three repeats. Significant differences are analyzed with two-way ANOVA (followed by a Holm-Sidak test), and indicated by *, $p < 0.05$ among various ligands, by #, $p < 0.05$ between each shear and static groups, and by $, $p < 0.05$ between 1 and 10 dyne/cm^2 groups.

1077 and -1119, Sigma-Aldrich) at 700×*g* for 30 min. The PMNs were obtained from the interface between Histopaque-1077 and -1119, washed with DPBS at 300×*g* for 10 min, and suspended in DPBS with 0.5% BSA on ice until use. The PMNs harvested from different mice were not combined to avoid abnormal immune response. The PMNs from same mouse were used randomly in 2–3 flow chamber assay in different cases to reduce individual differences. To detect the Ca^{2+} levels in cells, PMNs were loaded with 27.8 μg/ml Fluo-4-AM and 1 μg/ml Pluronic F-127 for 30 min on ice. After washing out extra dyes in suspension, the cells were incubated with 10 μg/ml isotype control or LFA-1 or Mac-1 blocking mAbs on ice for 20 min and then with fMLF of 1 μM in Hank's balanced salt solution (HBSS, 0.1% BSA) at room temperature (25–30 °C) for 10 min immediately before use.

2.3. Real-time fluorescent imaging of intracellular Ca^{2+} in PMNs

The intracellular Ca^{2+} levels were recorded during PMN adhesion and crawling at room temperature in a parallel plate flow chamber (GlycoTech, Gaithersburg, MD). The flow chamber was connected to a PHD22/2000 syringe pump (Harvard Apparatus, Holliston, MA) and counted on an automatic inverted microscope (IX81, Olympus, Tokyo, Japan) that was equipped with an electron-multiplying charge-coupled device (EMCCD) camera (897, Andor, Belfast, UK) controlled by the MetaMorph software (Universal Imaging, West Chester, PA) (Fig. 1A). The experiments were conducted at room temperature in order to keep the consistency of the experimental set-ups between intracellular Ca^{2+} imaging in this study and bond strength measurement in our previous work [19]. The low temperature may slow down the increase of Ca^{2+} influx and PMN adhesion, however, the incubation with fMLF at room temperature for 10 min is sufficient for Ca^{2+} signaling in PMNs to reach the maximum value [25–27]. A glass coverslip was incubated successively with anti-human IgG Fc pAbs (20 μg/ml), 1% BSA, and then ICAM-1, RAGE or JAM-A with Fc chimeras (5 μg/ml) for 1 h at 37 °C each. The washed coverslip was assembled onto the flow system and used as chamber substrate. 1.5 × 10^6 PMNs in 500 μl HBSS were injected into the chamber and incubated for 5 min without flow. Then a shear stress of 1 dyne/cm^2 was applied on the cells by perfusing HBSS (0.1% BSA, with Ca^{2+} and Mg^{2+}) for 10 min and 10 dyne/cm^2 for another 10 min. The two typical shear stresses were chosen, simply because PMN recruitment usually occurs at postcapillary venules where the shear stress is measured to be 1–10 dyne/cm^2 [28]. The dye-stained PMNs were excited by a 100-W xenon lamp through a 480AF30 filter (Omega Optical Inc., Brattleboro, VT) and the fluorescent images (Fig. 1B) from three field-of-views (FOVs) were recorded through a 40 × /NA0.95 objective lens and a filter of 520–560 nm at an interval of 20 s to visualize the Ca^{2+} oscillation in PMNs. Since the changes in Ca^{2+} signaling in individual PMNs were observed at a 500-ms interval in our previous work [16] and the Ca^{2+} spikes ranged from 40 s to several minutes, the sampling rate of 20 s given here was sufficient to collect most of the Ca^{2+} spikes.

2.4. Image processing and data analysis

Fluorescent images were analyzed using ImageJ software (National Institutes of Health, Bethesda, MD) to measure the intracellular Ca^{2+} levels in PMNs. For each adherent cell within the FOV, the mean fluorescence intensity (F_t) was obtained by subtracting acquired Ca^{2+} signals by background signals frame-by-frame and the lowest F_t from time-lapsed images was denoted as baseline fluorescence intensity F_0. The normalized ratio of F_t/F_0 was defined as relative fluorescence intensity (*RFI*) to reflect the intracellular Ca^{2+} changes (Fig. 1C). A *RFI* threshold value of 1.5 was set in this work to define those remarkable Ca^{2+} spikes in PMNs [29]. A spike with a peak value more than 1.5 was denoted as a specific event. The number of spiking Ca^{2+} peaks and the maximum value (peak value) of *RFI* was recorded in each case to represent the changes in Ca^{2+} signal.

2.5. Statistical analysis

Data were presented as the mean ± SEM. Significant differences among multiple groups were identified by two-way analysis of variance (ANOVA), followed by a Holm-Sidak test. *P* values less than 0.05 were considered statistically significant.

3. Results

3.1. Ca^{2+} transients in adherent PMNs on various ligands

To evaluate whether diverse ligand binding affects the β_2 integrin-mediated Ca^{2+} transients, we imaged in real time the time courses of Ca^{2+} oscillation in PMNs loaded with Fluo-4 during LFA-1– or Mac-1–ligand binding (Fig. 1A) and compared the capabilities of three typical ligands, ICAM-1, RAGE and JAM-A, to trigger the intracellular Ca^{2+} signaling (Fig. 2). Since low-affinity LFA-1 could not induce Ca^{2+} flux [11], we stimulated PMNs with fMLF to mimic *in vivo* inflammation microenvironment, activate PMN adhesion and enhance the fraction of high-affinity integrins and the baseline level of Ca^{2+}. No control experiments in the absence of fMLF were performed since the unstimulated PMNs could not adhere to the ligand-coated chamber substrate (data not shown). Fig. 1B and C displayed typical time-lapsed Ca^{2+} transients in a single PMN, exhibiting several Ca^{2+} spikes within a 10-min duration. The spike number and peak value of Ca^{2+} transients derived from the *RFI*–time curve were plotted against each ligand type to analyze their capabilities in inducing Ca^{2+} response (Fig. 2). Data indicated that the Ca^{2+} transients triggered by ICAM-1 binding under static condition are comparable to that of RAGE binding and the capability of JAM-A to mediate Ca^{2+} transients under static condition is lowest among the three ligands.

Physiological-like shear stress in the range between 1 and 10 dyne/cm^2 is reported to regulate integrin activation and subsequent Ca^{2+} flux [11,30]. The results showed that low shear stress (1 dyne/cm^2) augments significantly both the spike number (Fig. 2A) and peak value

(Fig. 2B) of Ca^{2+} transients induced by ICAM-1 or JAM-A, probably by inducing more high-affinity β_2 integrins and opening up mechanosensitive Ca^{2+} channels [17]. However, the peak value of Ca^{2+} transients return to the static level under high shear stress (10 dyne/cm^2), likely stemming from dissociation of β_2 integrin-ligand bonds or shear-induced cleavage of β_2 integrins from cell surface [31]. RAGE-mediated Ca^{2+} transients exhibit a shear-independent feature, implying a less effective impact of integrin-RAGE bonds on mechanotransduction. Collectively, distinct features of Ca^{2+} transients were uncovered for these ligands, suggesting their diverse roles in regulating PMN recruitment.

3.2. Role of LFA-1– or Mac-1–ICAM-1 engagement in triggering Ca^{2+} transients

ICAM-1 is the most effective and widely tested ligand for mediating PMN adhesion and transmigration [3,32–35]. LFA-1 and Mac-1 play distinct functions that LFA-1 initiates slow rolling and firm adhesion but Mac-1 mediates cell crawling in PMN recruitment when binding to ICAM-1. These distinct functions are governed by their different binding capacities and mechanical strengths [36–38]. Here the capabilities of LFA-1–ICAM-1 and Mac-1–ICAM-1 interactions to induce Ca^{2+} transients were compared by pre-incubating PMNs with *anti*-LFA-1 or anti-Mac-1 blocking mAbs respectively (Fig. 3). Data indicated that LFA-1 dominates the Ca^{2+} spike number triggered by ICAM-1 binding under static condition (Fig. 3A) and the peak value of Ca^{2+} transients tends to decrease after LFA-1 or Mac-1 blocking (Fig. 3B), even not significantly. At low shear stress, LFA-1 and Mac-1 compensate each other in the resulted Ca^{2+} spike number (Fig. 3A) and play equal roles in the peak value of Ca^{2+} transients (Fig. 3B). At high shear stress, only LFA-1 blocking reduces ICAM-1-mediated Ca^{2+} response significantly (Fig. 3), implying a crucial role of LFA-1–ICAM-1 bonds in triggering Ca^{2+} signal under high shear stress.

3.3. Role of LFA-1– or Mac-1–RAGE engagement in triggering Ca^{2+} transients

RAGE engages in thioglycollate- or trauma-induced leukocyte recruitment mainly through Mac-1 binding [39,40]. Here the results indicated that LFA-1 and Mac-1 work cooperatively in mediating Ca^{2+} spiking induced by RAGE binding under static condition (Fig. 4A), where only the role of Mac-1–RAGE binding is significant for the peak value of Ca^{2+} transients (Fig. 4B). LFA-1 blocking can increase the spike number under shear flow presumably by compensating more Mac-1–RAGE bonds instead (Fig. 4A). Accordingly, Mac-1 blocking reduces significantly the peak value of Ca^{2+} transients triggered by RAGE under shear flow (Fig. 4B) and also decreases the spike number at high shear stress (Fig. 4A), suggesting Mac-1–RAGE bonds play a more effective role in mediating Ca^{2+} response.

3.4. Role of LFA-1– or Mac-1–JAM-A engagement in triggering Ca^{2+} transients

JAM-A mainly locates at endothelial junctions and promotes PMN transmigration by interacting with LFA-1 [41,42]. Here the data indicated that the spike number and peak value of Ca^{2+} transients triggered by JAM-A binding under static condition is lowest among all the non-blocking groups (Fig. 2). LFA-1 blocking cannot further reduce the static Ca^{2+} response in PMNs on JAM-A, while Mac-1 blocking increases the spike number significantly and the peak value slightly (even not significantly) probably due to the formation of more LFA-1–JAM-A bonds (Fig. 5). When Ca^{2+} transients triggered by JAM-A binding are enhanced by low shear stress, LFA-1 and Mac-1 compensate each other in the spike number, presenting the null effect of β_2 integrin blocking (Fig. 5A). Meanwhile, LFA-1 dominates the peak value of Ca^{2+} oscillation (Fig. 5B). At high shear stress, LFA-1 blocking decreases Ca^{2+} response in PMNs on JAM-A moderately, while Mac-1 blocking increases the number of Ca^{2+} spikes by compensating more LFA-1–JAM-A bonds.

4. Discussion

Intracellular Ca^{2+} signaling is highly mechanosensitive and modulated by various mechanical stimuli. Shear stress enhances and quickens the cytoplasmic Ca^{2+} bursting of PMNs on immobilized E− or P-selectins [43,44], initiates Ca^{2+} influx mediated by transient receptor potential vallinoid type 4 (TRPV4) channel [45], primary cilium [46] or mitochondrial ATP [47] of ECs, and triggers a longitudinally-propagating, global Ca^{2+} wave *via* activation of purinergic signaling in atrial myocytes [48]. Stretch induces Ca^{2+} influx in vascular smooth muscle cells through plasma membrane stretch-activated channels (SACs) [49], increases Ca^{2+} spark in cardiomyocytes upon a mechanism that requires cytoskeletal integrity [50], and evokes Piezo1-dependent Ca^{2+} signaling and ATP release in urothelial cell [51]. Extracellular matrix stiffness modulates Ca^{2+} signaling of ECs in response to vascular endothelial growth factor (VEGF) [52], while mechanical vibration causes global Ca^{2+} response in ECs [53]. Evidently, significant alterations in Ca^{2+} signaling induced by mechanotransduction may be involved in many of physiological and pathological responses.

Mechanotransduction-induced Ca^{2+} signaling is modulated by the mechanical features of receptor-ligand interactions. Catch bonds formed between T cell receptor (TCR) and agonist peptide-major histocompatibility complex (pMHC) trigger Ca^{2+} signaling in T cells, whereas slip bonds formed between TCR and antagonist pMHC fail to activate [54]. High-affinity LFA-1 is necessary for the amplification of Ca^{2+} flux in the presence of shear flow, while low-affinity LFA-1 could not induce Ca^{2+} responses [11]. Therefore, bond strength might be critical to mechanical stimuli-induced Ca^{2+} signaling. In this study, we attempted to correlate the mechanical strength of LFA-1 or Mac-1 to respective ligands with their capabilities in inducing Ca^{2+} signaling in PMNs. LFA-1 dominates Ca^{2+} transients in adherent PMNs on ICAM-1

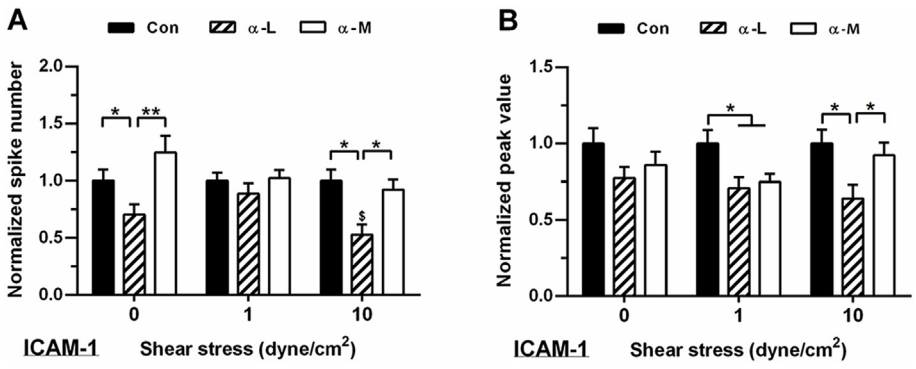

Fig. 3. Role of LFA-1- or Mac-1-ICAM-1 engagement in triggering Ca^{2+} transients under static or shear flow conditions. Normalized Ca^{2+} spike number (*A*) and peak value of RFI (*B*) in PMNs pretreated with isotype-matched control (Con) or LFA-1 (α-L) or Mac-1 (α-M) blocking mAbs on ICAM-1. Data are presented as the mean ± SEM from a total of 31–59 cells in 12 FOVs of three repeats and normalized by the mean value from control group. Significant differences are analyzed with two-way ANOVA (followed by a Holm-Sidak test), and indicated by *, $p < 0.05$; **, $p < 0.01$ among antibody-treated groups, and by $^{\$}$, $p < 0.05$ between 1 and 10 dyne/cm^2 groups.

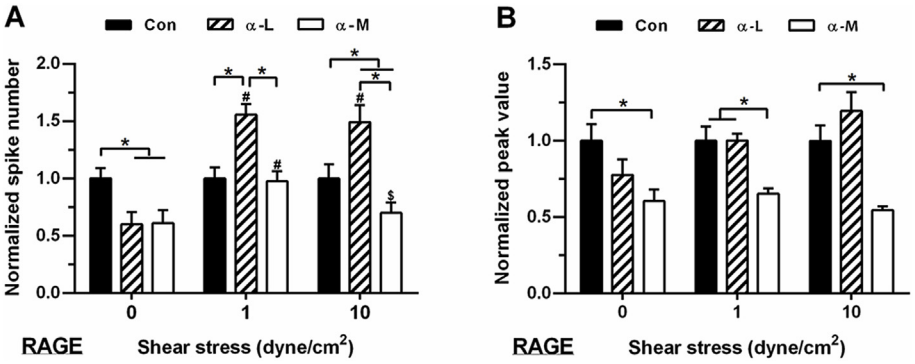

Fig. 4. Role of LFA-1- or Mac-1-RAGE engagement in triggering Ca^{2+} transients under static or shear flow conditions. Normalized Ca^{2+} spike number (*A*) and peak value of RFI (*B*) in PMNs pretreated with isotype-matched control (Con) or LFA-1 (α-L) or Mac-1 (α-M) blocking mAbs on RAGE. Data are presented as the mean ± SEM from a total of 23–42 cells in 12 FOVs of three repeats and normalized by the mean value from control group. Significant differences are analyzed with two-way ANOVA (followed by a Holm-Sidak test), and indicated by *, $p < 0.05$ among antibody-treated groups, by #, $p < 0.05$ between each shear and static groups, by $, $p < 0.05$ between 1 and 10 dyne/cm^2 groups.

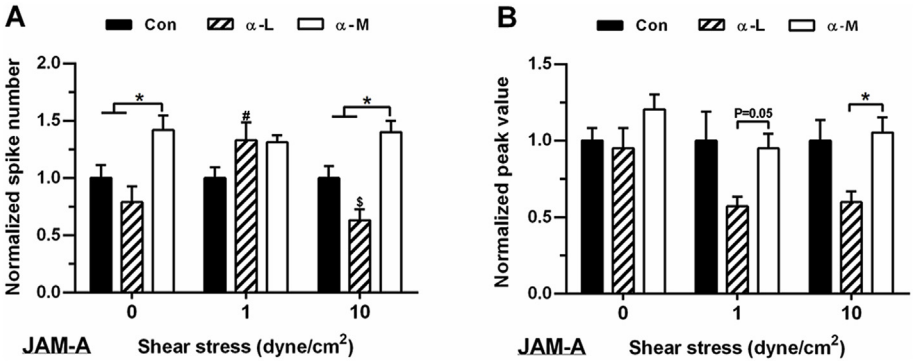

Fig. 5. Role of LFA-1 or Mac-1-JAM-A engagement in triggering Ca^{2+} transients under static or shear flow conditions. Normalized Ca^{2+} spike number (*A*) and peak value of RFI (*B*) in PMNs pretreated with isotype-matched control (Con) or LFA-1 (α-L) or Mac-1 (α-M) blocking mAbs on JAM-A. Data are presented as the mean ± SEM from a total of 18–47 cells in 12 FOVs of three repeats and normalized by the mean value from control group. Significant differences are analyzed with two-way ANOVA (followed by a Holm-Sidak test), and indicated by *, $p < 0.05$ among antibody-treated groups, by #, $p < 0.05$ between each shear and static groups, by $, $p < 0.05$ between 1 and 10 dyne/cm^2 groups.

(Fig. 3) and JAM-A (Fig. 5) while Mac-1 mediates Ca^{2+} transients induced by RAGE binding (Fig. 4), all of which are consistent with their bond strengths and their functions in PMN recruitment *in vivo* [19,39,42]. Our data correlate the mechanical strength of LFA-1– or Mac-1–ligand bonds with their capabilities to induce Ca^{2+} transients in PMNs. Higher bond strength gives rise to stronger Ca^{2+} response especially under physiological-like shear flow.

ICAM-1, RAGE and JAM-A are typical ligands for LFA-1 and Mac-1. Binding of LFA-1 and Mac-1 to ICAM-1 is essential for initiating classic recruitment cascade and maximizing Ca^{2+} signaling in PMNs [7]. Here we demonstrated that high-affinity LFA-1 bonds promotes greater Ca^{2+} response than Mac-1 bonds (Fig. 3), similar to the previous observation in the literature [11]. RAGE is known to interact with advanced glycation end products (AGEs) and reduce the cardiomyocyte Ca^{2+} transients in an dose-dependent manner [55]. Few works have reported Ca^{2+} transients triggered by the engagement of β_2 integrin to RAGE or JAM-A. Specifically, JAM-A locates onto both the endothelial tight junctions and the surfaces of PMNs [56], therefore JAM-A expressed on PMNs might engage in homophilic binding with those JAM-As coated on the chamber substrate in this study (Fig. 5). The homophilic interactions could also initiate the Ca^{2+} transients in PMNs triggered by JAM-A binding, which might lead to the abnormal increase of Ca^{2+} spike number after Mac-1 blocking (Fig. 5A).

Collectively, we focus in this study on the contributions of bond mechanical strength in triggering Ca^{2+} signaling, which provides an insight into the mechanotransduction and outside-in signaling of PMN recruitment. It should also be mentioned that the downstream signaling of LFA-1 or Mac-1-mediated Ca^{2+} transients may not be the same for distinct ligands. One possibility is that LFA-1 and Mac-1 utilize different calcium-dependent kinases to trigger adherent activation and migration of PMNs.

This *in vitro* study applied a flow chamber assay to mimic PMN recruitment during inflammation and gave a brief description of the Ca^{2+} transients in PMNs triggered by distinct ligands under physiological-like shear flow. However, the expression and distribution of multiple ligands are tissue- and stimulus-specific. The matrix stiffness, vessel geometry and blood hemodynamics in different tissues complicate the microenvironment faced by PMNs *in vivo*. Therefore, the Ca^{2+} responses of PMNs in specialized *in vivo* microenvironment might be different and need further investigation.

Declarations of interest

The authors declare no conflicts of interest, financial or otherwise.

CRediT authorship contribution statement

Xinyu Shu: Conceptualization, Investigation, Visualization. **Ning Li:** Conceptualization, Validation, Writing - original draft, Data curation, Writing - review & editing. **Dandan Huang:** Methodology. **Yan Zhang:** Writing - review & editing. **Shouqin Lü:** Writing - review & editing. **Mian Long:** Conceptualization, Writing - review & editing, Supervision.

Acknowledgments

This work was supported by National Natural Science Foundation of China Grants 91642203, 31661143044, 31627804 and 31870930, and Strategic Priority Research Program and Frontier Science Key Project of Chinese Academy of Sciences grants QYZDJ-SSW-JSC018 and XDB22040101.

References

[1] K. Hübner, I. Surovtsova, K. Yserentant, M. Hänsch, U. Kummer, Ca^{2+} dynamics correlates with phenotype and function in primary human neutrophils, Biophys. Chem. 184 (2013) 116–125, https://doi.org/10.1016/j.bpc.2013.09.006.
[2] R. Alon, M.L. Dustin, Force as a facilitator of integrin conformational changes during leukocyte arrest on blood vessels and antigen-presenting cells, Immunity 26 (2007) 17–27, https://doi.org/10.1016/j.immuni.2007.01.002.
[3] K. Ley, C. Laudanna, M.I. Cybulsky, S. Nourshargh, Getting to the site of inflammation: the leukocyte adhesion cascade updated, Nat. Rev. Immunol. 7 (2007) 678–689, https://doi.org/10.1038/nri2156.
[4] N. Li, S.Q. Lü, Y. Zhang, M. Long, Mechanokinetics of receptor-ligand interactions

in cell adhesion, Acta Mech. Sin. 31 (2015) 248–258, https://doi.org/10.1007/s10409-015-0407-8.
[5] K. Buschmann, R. Tschada, M.S. Metzger, N. Braach, N. Kuss, H. Hudalla, J. Poeschl, D. Frommhold, RAGE controls leukocyte adhesion in preterm and term infants, BMC Immunol. 15 (2014) 53, https://doi.org/10.1186/s12865-014-0053-0.
[6] M.A. Hasan, W.G. Ahn, D.K. Song, N-acetyl-L-cysteine and cysteine increase intracellular calcium concentration in human neutrophils, Korean J. Physiol. Pharmacol. 20 (2016) 449–457, https://doi.org/10.4196/kjpp.2016.20.5.449.
[7] U.Y. Schaff, I. Yamayoshi, T. Tse, D. Griffin, L. Kibathi, S.I. Simon, Calcium flux in neutrophils synchronizes beta(2) integrin adhesive and signaling events that guide inflammatory recruitment, Ann. Biomed. Eng. 36 (2008) 632–646, https://doi.org/10.1007/s10439-008-9453-8.
[8] R.W. Beerman, M.A. Matty, G.G. Au, L.L. Looger, K.R. Choudhury, P.J. Keller, D.M. Tobin, Direct in vivo manipulation and imaging of calcium transients in neutrophils identify a critical role for leading-edge calcium flux, Cell Rep. 13 (2015) 2107–2117, https://doi.org/10.1016/j.celrep.2015.11.010.
[9] R. Immler, S.I. Simon, M. Sperandio, Calcium signalling and related ion channels in neutrophil recruitment and function, Eur. J. Clin. Investig. 48 (2018) e12964, , https://doi.org/10.1111/eci.12964.
[10] R.E. Roberts, M.B. Hallett, Neutrophil cell shape change: mechanism and signalling during cell spreading and phagocytosis, Int. J. Mol. Sci. 20 (2019) 1383, , https://doi.org/10.3390/ijms20061383.
[11] N. Dixit, I. Yamayoshi, A. Nazarian, S.I. Simon, Migrational guidance of neutrophils is mechanotransduced via high-affinity LFA-1 and calcium flux, J. Immunol. 187 (2011) 472–481, https://doi.org/10.4049/jimmunol.1004197.
[12] D. Eierman, C. Hellberg, A. Sjolander, T. Andersson, Chemotactic factor receptor activation transiently impairs the Ca^{2+} signaling capacity of beta 2 integrins on human neutrophils, Exp. Cell Res. 215 (1994) 90–96, https://doi.org/10.1006/excr.1994.1319.
[13] C. Hellberg, L. Molony, L. Zheng, T. Andersson, Ca^{2+} signalling mechanisms of the beta 2 integrin on neutrophils: involvement of phospholipase C gamma 2 and Ins (1,4,5)P3, Biochem. J. 317 (1996) 403–409, https://doi.org/10.1042/bj3170403.
[14] E.J. Pettit, M.B. Hallett, Pulsatile Ca^{2+} influx in human neutrophils undergoing CD11b/CD18 integrin engagement, Biochem. Biophys. Res. Commun. 230 (1997) 258–261, https://doi.org/10.1006/bbrc.1996.5931.
[15] N. Dixit, S.I. Simon, Chemokines, selectins and intracellular calcium flux: temporal and spatial cues for leukocyte arrest, Front. Immunol. 3 (2012) 188, https://doi.org/10.3389/fimmu.2012.00188.
[16] Y.H. Xu, D.D. Huang, S.Q. Lü, Y. Zhang, M. Long, Mechanical features of endothelium regulate cell adhesive molecule-induced calcium response in neutrophils, APL Bioeng. 3 (2019) 016104, , https://doi.org/10.1063/1.5045115.
[17] N. Dixit, M.H. Kim, J. Rossaint, I. Yamayoshi, A. Zarbock, S.I. Simon, LFA-1, kindlin-3 and calcium flux orchestrate neutrophil recruitment during inflammation, J. Immunol. 189 (2012) 5954–5964, https://doi.org/10.4049/jimmunol.1201638.
[18] S.I. Simon, M.R. Sarantos, C.E. Green, U.Y. Schaff, Leucocyte recruitment under fluid shear: mechanical and molecular regulation within the inflammatory synapse, Clin. Exp. Pharmacol. Physiol. 36 (2009) 217–224, https://doi.org/10.1111/j.1440-1681.2008.05083.x.
[19] N. Li, H. Yang, M.L. Wang, S.Q. Lü, Y. Zhang, M. Long, Ligand-specific binding forces of LFA-1 and Mac-1 in neutrophil adhesion and crawling, Mol. Biol. Cell 29 (2018) 408–418, https://doi.org/10.1091/mbc.E16-12-0827.
[20] Y. Du, N. Li, H. Yang, C.H. Luo, Y.X. Gong, C.F. Tong, Y.X. Gao, S.Q. Lü, M. Long, Mimicking liver sinusoidal structures and functions using a 3D-configured microfluidic chip, Lab Chip 17 (2017) 782–794, https://doi.org/10.1039/c6lc01374k.
[21] H. Yang, N. Li, Y. Du, C.F. Tong, S.Q. Lü, J.R. Hu, Y. Zhang, M. Long, Neutrophil adhesion and crawling dynamics on liver sinusoidal endothelial cells under shear flow, Exp. Cell Res. 351 (2017) 91–99, https://doi.org/10.1016/j.yexcr.2017.01.002.
[22] R. Boxio, C. Bossenmeyer-Pourié, N. Steinckwich, C. Dournon, O. Nüsse, Mouse bone marrow contains large numbers of functionally competent neutrophils, J. Leukoc. Biol. 75 (2004) 604–611, https://doi.org/10.1189/jlb.0703340.
[23] C.A. Lowell, L. Fumagalli, G. Berton, Deficiency of Src family kinases $p59/61^{hck}$ and $p58^{c\text{-}fgr}$ results in defective adhesion-dependent neutrophil functions, J. Cell Biol. 133 (1996) 895–910, https://doi.org/10.1083/jcb.133.4.895.
[24] M. Swamydas, M.S. Lionakis, Isolation, purification and labeling of mouse bone marrow neutrophils for functional studies and adoptive transfer experiments, J. Vis. Exp. 77 (2013) e50586, , https://doi.org/10.3791/50586.
[25] K. Wong, X.B. Li, Protein phosphatase inhibitors exert specific and nonspecific effects on calcium influx in thapsigargin-treated human neutrophils, Inflammation 22 (1998) 631–642, https://doi.org/10.1023/a:1022318631686.
[26] A. Kasorn, P. Alcaide, Y. Jia, K.K. Subramanian, B. Sarraj, Y. Li, F. Loison, H. Hattori, L.E. Silberstein, W.F. Luscinskas, H.R. Luo, Focal adhesion kinase regulates pathogen-killing capability and life span of neutrophils via mediating both adhesion-dependent and -independent cellular signals, J. Immunol. 183 (2009) 1032–1043, https://doi.org/10.4049/jimmunol.0802984.
[27] E.B. Lomakina, R.E. Waugh, Signaling and dynamics of activation of LFA-1 and Mac-1 by immobilized IL-8, Cell. Mol. Bioeng. 3 (2010) 106–116, https://doi.org/10.1007/s12195-009-0099-x.T.
[28] N. Heisig, Functional analysis of microcirculation in the exocrine pancreas, Adv. Microcirc. 1 (1968) 89–94.
[29] H. Ohata Miyazaki, M. Yamamoto, K. Momose, Spontaneous and flow-induced Ca^{2+} transients in retracted regions in endothelial cells, Biochem. Biophys. Res. Commun. 281 (2001) 172–179, https://doi.org/10.1006/bbrc.2001.4331.
[30] D. Frommhold, A. Kamphues, I. Hepper, M. Pruenster, I.K. Lukic, I. Socher, V. Zablotskaya, K. Buschmann, B. Lange-Sperandio, J. Schymeinsky, E. Ryschich, J. Poeschl, C. Kupatt, P.P. Nawroth, M. Moser, B. Walzog, A. Bierhaus, M. Sperandio, RAGE and ICAM-1 cooperate in mediating leukocyte recruitment during acute inflammation in vivo, Blood 116 (2010) 841–849, https://doi.org/10.1182/blood-2009-09-244293.
[31] A. Makino, H.Y. Shinb, Y. Komai, S. Fukuda, M. Coughlin, M. Sugihara-Seki, G.W. Schmid-Schönbein, Mechanotransduction in leukocyte activation: a review, Biorheology 44 (2007) 221–249.
[32] H.Y. Shin, S.I. Simon, G.W. Schmid-Schoenbein, Fluid shear-induced activation and cleavage of CD18 during pseudopod retraction by human neutrophils, J. Cell. Physiol. 214 (2008) 528–536, https://doi.org/10.1002/jcp.21235.
[33] R. Gorina, R. Lyck, D. Vestweber, B. Engelhardt, Beta(2) Integrin-mediated crawling on endothelial ICAM-1 and ICAM-2 is a prerequisite for transcellular neutrophil diapedesis across the inflamed blood–brain barrier, J. Immunol. 192 (2014) 324–337, https://doi.org/10.4049/jimmunol.1300858.
[34] C.Z. Wang, N. Li, C. Zhang, S.J. Sun, Y.X. Gao, M. Long, Effects of simulated microgravity on functions of neutrophil-like HL-60 cells, Microgravity Sci. Technol. 27 (2015) 515–527, https://doi.org/10.1007/s12217-015-9473-6.
[35] X. Zhang, L.D. Li, N. Li, X.Y. Shu, L.W. Zhou, S.Q. Lü, S.B. Chen, D.B. Mao, M. Long, Salt bridge interactions within the beta(2) integrin alpha(7) helix mediate force-induced binding and shear resistance ability, FEBS J. 285 (2018) 261–274, https://doi.org/10.1111/febs.14335.
[36] C.F. Tong, Y. Zhang, S.Q. Lü, N. Li, Y.X. Gong, H. Yang, S.L. Feng, Y. Du, D.D. Huang, M. Long, Binding of intercellular adhesion molecule 1 to beta(2)-integrin regulates distinct cell adhesion processes on hepatic and cerebral endothelium, Am. J. Physiol. Cell Physiol. 315 (2018) C409–C421, https://doi.org/10.1152/ajpcell.00083.2017.
[37] D.B. Mao, S.Q. Lü, N. Li, Y. Zhang, M. Long, Conformational stability analyses of alpha subunit I domain of LFA-1 and Mac-1, PLoS One 6 (2011) e24188, , https://doi.org/10.1371/journal.pone.0024188.
[38] N. Li, D.B. Mao, S.Q. Lü, C.F. Tong, Y. Zhang, M. Long, Distinct binding affinities of Mac-1 and LFA-1 in neutrophil activation, J. Immunol. 190 (2013) 4371–4381, https://doi.org/10.4049/jimmunol.1201374.
[39] N. Li, X. Zhang, P.W. Li, H. Yang, C.F. Tong, S.Q. Lü, Y. Zhang, Z.Y. Ye, J. Pan, M. Long, Mechanical strength and structural basis of beta(2) integrin to mediate neutrophil accumulation on liver sinusoidal endothelial cells: a study using atomic force microscopy and molecular dynamics simulations, CMES-Comp. Model. Eng. Sci. 116 (2018) 263–279, https://doi.org/10.31614/cmes.2018.04079.
[40] T. Chavakis, A. Bierhaus, N. Al-Fakhri, D. Schneider, S. Witte, T. Linn, M. Nagashima, J. Morser, B. Arnold, K.T. Preissner, P.P. Nawroth, The pattern recognition receptor (RAGE) is a counterreceptor for leukocyte integrins: a novel pathway for inflammatory cell recruitment, J. Exp. Med. 198 (2003) 1507–1515, https://doi.org/10.1084/jem.20030800.
[41] H. Ozaki, K. Ishii, H. Horiuchi, H. Arai, T. Kawamoto, K. Okawa, A. Iwamatsu, T. Kita, Cutting edge: combined treatment of TNF-alpha and IFN-gamma causes redistribution of junctional adhesion molecule in human endothelial cells, J. Immunol. 163 (1999) 553–557.
[42] G. Ostermann, K.S.C. Weber, A. Zernecke, A. Schroder, C. Weber, JAM-1 is a ligand of the beta(2) integrin LFA-1 involved in transendothelial migration of leukocytes, Nat. Immunol. 3 (2002) 151–158, https://doi.org/10.1038/ni755.
[43] B. Huang, Y.C. Ling, J.G. Lin, X. Du, Y. Fang, J.H. Wu, Force-dependent calcium signaling and its pathway of human neutrophils on P-selectin in flow, Protein Cell 8 (2017) 103–113, https://doi.org/10.1007/s13238-016-0364-4 (2017).
[44] L. Zhang, J.H. Wu, Y. Fang, E-selectin mediated-calcium response of neutrophils under fluid shear stresses, J. Med. Biomechanics 33 (2018) 150–156.
[45] S.A. Mendoza, J. Fang, D.D. Gutterman, D.A. Wilcox, A.H. Bubolz, R.S. Li, M. Suzuki, D.X. Zhang, TRPV4-mediated endothelial Ca^{2+} influx and vasodilation in response to shear stress, Am. J. Physiol. Heart Circ. Physiol. 298 (2010) H466–H476, https://doi.org/10.1152/ajpheart.00854.2009.
[46] S.M. Nauli, Y. Kawanabe, J.J. Kaminski, W.J. Pearce, D.E. Ingber, J. Zhou, Endothelial cilia are fluid shear sensors that regulate calcium signaling and nitric oxide production through polycystin-1, Circulation 117 (2008) 1161–1171, https://doi.org/10.1161/CIRCULATIONAHA.107.710111.
[47] K. Yamamoto, H. Imamura, J. Ando, Shear stress augments mitochondrial ATP generation that triggers ATP release and Ca^{2+} signaling in vascular endothelial cells, Am. J. Physiol. Heart Circ. Physiol. 315 (2018) H1477–H1485, https://doi.org/10.1152/ajpheart.00204.2018.
[48] J.C. Kim, S.H. Woo, Shear stress induces a longitudinal Ca^{2+} wave via autocrine activation of P2Y(1) purinergic signalling in rat atrial myocytes, J. Physiol. 593 (2015) 5091–5109, https://doi.org/10.1113/JP271016.
[49] G. Gilbert, T. Ducret, R. Marthan, J.P. Savineau, J.F. Quignard, Stretch-induced Ca^{2+} signalling in vascular smooth muscle cells depends on Ca^{2+} store segregation, Cardiovasc. Res. 103 (2014) 313–323, https://doi.org/10.1093/cvr/cvu069.
[50] G. Iribe, C.W. Ward, P. Camelliti, C. Bollensdorff, F. Mason, R.A.B. Burton, A. Garny, M.K. Morphew, A. Hoenger, W.J. Lederer, P. Kohl, Axial stretch of rat single ventricular cardiomyocytes causes an acute and transient increase in Ca^{2+} spark rate, Circ. Res. 104 (2009) 787–795, https://doi.org/10.1161/CIRCRESAHA.108.193334.
[51] T. Miyamoto, T. Mochizuki, H. Nakagomi, S. Kira, M. Watanabe, Y. Takayama, Y. Suzuki, S. Koizumi, M. Takeda, M. Tominaga, Functional role for Piezo1 in stretch-evoked Ca^{2+} influx and ATP release in urothelial cell cultures, J. Biol. Chem. 289 (2014) 16565–16575, https://doi.org/10.1074/jbc.M113.528638.
[52] K.E. Derricks, V. Trinkaus-Randall, M.A. Nugent, Extracellular matrix stiffness modulates VEGF calcium signaling in endothelial cells: individual cell and population analysis, Integr. Biol. 7 (2015) 1011–1025, https://doi.org/10.1039/c5ib00140d.
[53] W.S. Nishitani, T.A. Saif, Y.X. Wang, Calcium signaling in live cells on elastic gels under mechanical vibration at subcellular levels, PLoS One 6 (2011) e26181, ,

https://doi.org/10.1371/journal.pone.0026181 (2011).
[54] B.Y. Liu, W. Chen, B.D. Evavold, C. Zhu, Accumulation of dynamic catch bonds between TCR and agonist peptide-MHC triggers T cell signaling, Cell 157 (2014) 357–368, https://doi.org/10.1016/j.cell.2014.02.053.
[55] Z. Hegab, T.M.A. Mohamed, N. Stafford, M. Mamas, E.J. Cartwright, D. Oceandy, Advanced glycation end products reduce the calcium transient in cardiomyocytes by increasing production of reactive oxygen species and nitric oxide, FEBS Open Bio 7 (2017) 1672–1685, https://doi.org/10.1002/2211-5463.12284.
[56] J.S. Khandoga, H. Kessler, M. Meissner, M. Hanschen, T. Corada, G. Motoike, E. Enders, F. Dejana, Krombach, Junctional adhesion molecule-A deficiency increases hepatic ischemia-reperfusion injury despite reduction of neutrophil transendothelial migration, Blood 106 (2005) 725–733, https://doi.org/10.1182/blood-2004-11-4416.